Insertion and Partition of Sodium Taurocholate into Egg Phosphatidylcholine Vesicles

Karine Andrieux,[1,2] Laura Forte,[1] Sylviane Lesieur,[1] Maité Paternostre,[1] Michel Ollivon,[1] and Cécile Grabielle-Madelmont[1]

Received March 8, 2004; accepted April 9, 2004

Purpose. To get a continuous description of the insertion and partition processes of sodium taurocholate (TC) into the lipid bilayers of vesicles that can serve as a model for understanding the mechanism of destabilization by the bile salts of liposomes used as drug carriers for oral administration.

Methods. The progressive solubilization of egg phosphatidylcholine vesicles during TC addition at controlled rates was followed by continuous turbidity (OD) and resonance energy transfer (RET) between two fluorescent probes. The influence of the lipid and TC concentrations as well as the rate of TC addition on the processes were examined.

Results. Continuous turbidity recordings allowed following of the size and composition evolutions of the mixed TC/lipid aggregates formed at different steps of the vesicle-micelle transition. The solubilization mechanism is governed by complex kinetics that depend on the surfactant concentration and its addition rate. A two-step process characterizes the evolution of the vesicular state: interaction of TC molecules with the external monolayer of the vesicles first occurs. The homogeneous distribution of TC within the lipid matrix after its insertion is a very slow process. A micellar structural reorganization is observed when TC is added rapidly.

Conclusions. This work provides detailed information on the slow insertion and diffusion kinetics of TC in liposomal bilayers by using a dynamic study which mimics physiological phenomena of digestion.

KEY WORDS: bile salts; liposome; turbidity; kinetics; fluorescence.

INTRODUCTION

Liposomes can be used as drug carriers for oral administration of pharmaceutical products (1). Among the different procedures of liposome preparation, the technique based on detergent removal from mixed detergent/phospholipid micelles comparatively to classical techniques using organic solvents offers the advantages of avoiding the presence of residual solvent or the possible alteration of the labile drugs (2). Choosing a surfactant like sodium taurocholate (TC) enables obtaining of biocompatible liposomal carriers even if a small amount of TC persists. After oral administration, liposomes and other organized systems are solubilized under physiological conditions in the gastrointestinal tract by bile salts (BS) (3). The liposomes are also models of biological membranes to perform protein reconstitution or to mimic membrane barriers (4).

Solubilizing surfactants (called also detergents) are known to induce membrane permeability enhancement, which leads to increase drug absorption through intestinal wall (5) and transdermal penetration (6). Solubilization of liposomes by detergent is due to the insertion of surfactant molecules in the lipid shell to form new aggregates. The different steps of the transformation of lipidic vesicles into mixed micelles through addition of surfactant refer to the vesicle-micelle transition (Fig. 1) (7). Effects of bile salts on lipid vesicles have been investigated by a number of techniques such as light scattering (8–11), fluorescence measurements (11), cryotransmission electron microscopy (12), permeability studies (13,14), X-ray diffraction (15,16), differential scanning calorimetry (DSC) (17), and time-resolved static and dynamic light and small-angle neutron scattering (18).

Light scattering or turbidity measurements are direct methods that allow following of the vesicle solubilization and the micelle formation mainly because of the gap between the mean sizes of these two types of aggregates. Indeed, vesicles are large particles with high turbidity, whereas micelles are small ones, which then weakly scatter the light. More generally, any process that involves a change of morphology (size and shape) or number of particles yields a change in turbidity of the sample. Accordingly, the vesicle-micelle transition and the phenomena of aggregation and aggregate fusion that can occur along this transition result in optical density changes (4,19). The vesicle-micelle transition is usually described in three stages delimited by two phase limits represented by the lines arbitrary called B and C in Fig. 1 (7). In the first step, the detergent molecules partition between the lipid bilayers and the aqueous medium (Fig. 1, vesicular domain below line B). The vesicular domain is characterized by a high optical density (OD). The insertion of detergent into the lipid membrane induces evolution of the detergent-loaded vesicles in equilibrium with a specific detergent concentration in the aqueous medium without disrupting the lipid bilayers. The second step (Fig. 1, between lines B and C) corresponds to a coexistence domain for which the saturation of the phospholipidic bilayers by the surfactant molecules (phase limit B) leads to a progressive solubilization of the liposomes into lipid-detergent mixed micelles inducing a drastic decrease in OD. The third step concerns the complete membrane solubilization into mixed micelles (phase limit C), which results in a clear solution of very low OD (Fig. 1, micellar domain above line C). The use of continuous light scattering recordings during the continuous addition of surfactant molecules to vesicle dispersions (20) allows (i) to precisely follow the occurrence and evolution of the successive intermediate aggregates, (ii) to accurately determine the limits of the main phase domains of the transition, (iii) to study the kinetics of insertion and distribution of the detergent in the aggregates during their formation. Only a continuous recording of the events gives account for the evolution of the morphology changes of the

[1] Equipe Physicochimie des Systèmes Polyphasés, UMR CNRS 8612, 92296 Châtenay-Malabry cedex, France.

[2] To whom correspondence should be addressed. (e-mail: karine.andrieux@cep.u-psud.fr)

ABBREVIATIONS: DPPC, dipalmitoylphosphatidylcholine; EPA, egg phosphatidic acid; EPC, egg phosphatidylcholine; LIP, lipid; NBD-PE, *N*-(7-nitro-2,1,3-benzoxadiazol-4-yl)-phosphatidylethanolamine; OD, optical density; OG, octylglucoside (*n*-octyl-β-D-glucopyranoside); QELS, quasi-elastic light scattering; R_e, TC/lipid molar ratio in the membrane; RET, resonance energy transfer; REV, large unilamellar vesicles; Rho-PE, *N*-(lissamine rhodamine B sulfonyl)-phosphatidylethanolamine; SUV, small unilamellar vesicles; TC, sodium taurocholate.

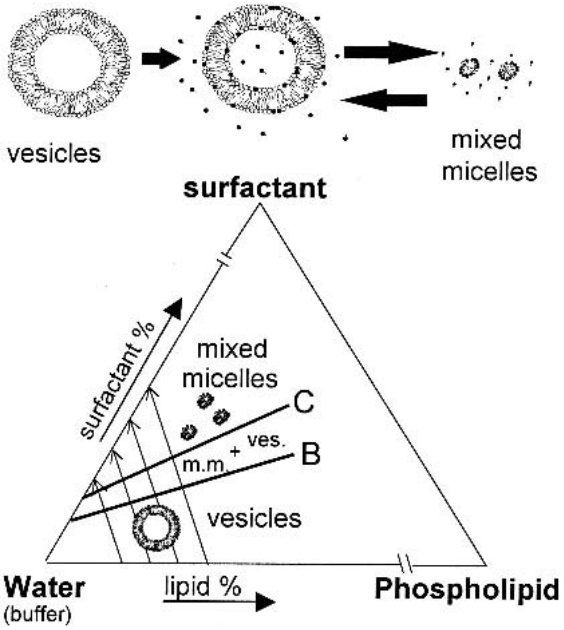

Fig. 1. Symbolic representation of the vesicle to micelle transition and schematic ternary phase diagram of phospholipid/surfactant/water mixtures. The pathway followed by the vesicle-micelle transition is shown by the arrows that cross a two-phase domain in which vesicles (ves.) and mixed micelles (m.m.) coexist. When the transition crosses this two-phase domain, the composition of the two phases is unchanged and only the proportions between them is varying. Straight lines noted B and C represent phase limits (see text).

surfactant/lipid aggregates occurring during the solubilization process. This methodology was already used to evidence that slow processes control interactions of bile salts with phospholipids (21). This first study was performed by addition to vesicles composed of egg phosphatidylcholine (EPC) and EPC/cholesterol (7/3) of high concentrations (30–200 mM) of TC at relatively high rates (0.08–3.1 μmol/min). It has been shown that the [TC]/[lipid] molar ratio corresponding to the micelle formation is strongly dependent on the rate of TC addition. The slow kinetics of TC organization into phospholipid bilayers have been confirmed by the long times required for dipalmitoylphosphatidylcholine (DPPC)-TC mixtures to reach equilibrium at 4°C as studied by X-ray diffraction (15).

Nevertheless, the mechanism of the vesicle-micelle transition of the TC/phospholipid system is not yet fully understood. In order to elaborate new vesicle formulations adequately resistant to bile salts after their oral administration, the process of liposome destabilization by the insertion and diffusion of the detergent molecules inside the phospholipid bilayers has to be elucidated.

In the current paper, the processes of interaction of sodium taurocholate with small unilamellar vesicles of egg phosphatidylcholine (EPC SUV) and large unilamellar vesicles of phosphatidylcholine/phosphatidic acid (EPC/EPA REV) were examined by a continuous turbidity analysis. The dependencies of the initial lipid concentration, the addition rates, and concentration of TC solutions on the mixed TC/lipid aggregate structure were investigated all along the vesicle-micelle transition. Information provided at a supramolecular level by turbidity measurements were completed by a study at a molecular level using fluorescence experiments based on resonance energy transfer (RET) (20,22).

MATERIALS AND METHODS

Materials

Egg phosphatidylcholine (EPC), *N*-(7-nitro-2,1,3-benzoxadiazol-4-yl)-phosphatidylethanolamine (NBD-PE), and *N*-(lissamine rhodamine B sulfonyl)-phosphatidylethanolamine (Rho-PE) were purchased from Avanti (Alabaster, AL, USA). Egg phosphatidic acid (EPA), *N*-[2-hydroxyethyl] piperazine-*N*'-[2-ethane sulfonic acid] (HEPES), sodium chloride (NaCl), and sodium taurocholate (TC) were obtained from Sigma (St. Louis, MO, USA). The buffer consisted of 10 mM HEPES and 145 mM NaCl, adjusted to pH 7.4.

Vesicle Preparation

Small unilamellar liposomes of EPC, noted EPC SUV, were prepared from a thin film of pure EPC obtained by evaporation of a chloroform solution of the lipids under a nitrogen stream followed by lyophilization for 12 h. The dried film was hydrated with buffer (23). The lipid dispersions were ultrasonicated (Vibracell Sonifer, Sonica et Matérials, 500 W, VWR International, Strasbourg, France) during 6 cycles of 2 min at 1 min intervals under a nitrogen atmosphere in an ice bath to maintain the temperature in the flask around 4°C. Then, the vesicles were centrifuged and filtered through a 0.22-μm filter to remove metal particles from the ultrasonic tip. After 2 days of storage, the SUV were partly aggregated (24). QELS indicated an apparent mean diameter of 107 ± 15 nm. The unit size of the vesicles remains around 25 nm in diameter. This state of aggregation and the mean diameter remained stable over the time of the experiments (3–4 days).

Large unilamellar vesicles composed of EPC and EPA (EPC/EPA 90/10 w/w), noted EPC/EPA REV, were prepared by the reverse-phase evaporation technique (25) followed by a sequential extrusion (Extruder Lipex Biomembranes, Vancouver, Canada) down through polycarbonate membranes (Nuclepore) of 0.8, 0.4, 0.2, 0.1, and 0.05 μm diameter. EPC/EPA REV so obtained are stable over several months at 4°C thanks to the repulsive effect of the negatively charged EPA (24). Between two experiments, REV vesicles were stored at 4°C to avoid lipid degradation. EPC/EPA REV containing NBD-PE and Rho-PE were prepared according to the same procedure. Each of the lipid fluorescent probes was added to the lipid solution in chloroform at a probe/lipid molar percentage of 1.6. Mean diameters of 140 ± 25 and 122 ± 40 nm were measured by QELS for the unlabeled and labeled vesicles, respectively.

Stock dispersions of vesicles (1.5 to 6 ml) were prepared at a lipid concentration of 20 or 40 mM. The phospholipid concentration was accurately determined by weight assuming densities equal to 1.

Determination of the TC Critical Micellar Concentration by Surface Tension Measurements

In literature data, there is a lack of agreement about the critical micellar concentration of TC (3), which is very sensitive to impurities in sample and aqueous electrolyte medium and also depends on the technique used and the treatment of the experimental data (26). As interaction of TC with lipid bilayers may differ upon addition of the surfactant at concen-

trations below or above its critical micellar concentration (CMC), we have determined its value in the buffer used in this study (145 mM NaCl, 10 mM HEPES, pH 7.4). First, we have controlled that the buffer was efficient to keep the pH at 7.4 ± 0.1 for solutions containing up to 100 mM of TC. Surface tension vs. the TC concentration was measured using a tensiometer (Krüss, Palaiseau, France; K10ST). The experimental data were interpreted according to the procedure described by Meguro *et al.* (27). A CMC value of 3.5 mg/ml (6.5 ± 0.5 mM) was obtained in agreement with the data (4–9 mM) found in 150 mM NaCl medium by measurement of self-diffusion coefficients and micellar solubilization (3). A similar value (6 mM in 150 mM NaCl medium) was obtained by Kratohvil *et al.* (26) from tension surface measurement, this value being not considered as a "true" CMC, as the presence of few aggregates of small size was observed below this value by light scattering.

Quasi-elastic Light Scattering

The mean hydrodynamic diameters (MD) of the vesicles were determined by quasi-elastic light scattering (QELS) by using a N4 Coultronics apparatus (Beckman Coulter, Roissy, France). The calculations were made according to the Stokes-Einstein equation assuming the particles to be independent and spherical. The mean diameter values correspond to the average of three measurements with a standard deviation lower than 5%.

Continuous Turbidity Measurements

The optical density of the lipid/detergent mixtures was continuously recorded by monitoring the turbidity at 350, 400, or 420 nm depending on the initial vesicles on a Perkin Elmer Lambda 2 double beam spectrophotometer (Perkin Elmer, Courtaboeuf, France) monitored by a computer, as previously described (20). The reference cuvette contained the buffer used for the vesicle preparation. A precision syringe (Hamilton, VWR International, Strasbourg, France) placed in a temperature-jacket mounted on a syringe pump (Braun Perfusor VI, Roucaire, France) was used to introduce, through a catheter, a TC solution of known concentration (9.95 or 20.0 mM) into a 1-cm optical quartz cuvette containing the vesicle dispersion (1.5 ml, $[LIP]_{ini}$ = 0.5 to 5 mM). The cuvettes were placed in a thermostated cell support in the spectrophotometer. The analyses were carried out at 25°C, at controlled rates of TC addition varying between 0.03 and 0.55 μmol/min and under a constant sample stirring. The experimental conditions (lipid and TC concentrations and rate of addition) are indicated in the figure legends. The signal was continuously recorded during the TC addition, and the time was converted to TC concentrations ([TC]) by using the following equation:

$$[TC]_{tot} = ([TC]_{syr}\ rt)/(V_{ini} + rt) \quad (1)$$

Where $[TC]_{tot}$ is the total concentration of TC in the cuvette at time t, $[TC]_{syr}$ is the concentration of the TC solution in the syringe, r is the addition rate of TC solution expressed as ml/s, and V_{ini} is the initial volume of the liposomal dispersion in the cuvette. The total lipid concentration $[LIP]_{tot}$ of the dispersion, which changes during the solubilization, due to dilution by the TC solution added, is given by the following equation:

$$[LIP]_{tot} = ([LIP]_{ini}\ V_{ini})/(V_{ini} + rt) \quad (2)$$

where $[LIP]_{ini}$ is the initial lipid concentration in the cuvette.

Determination of the breakpoints on the solubilization curves was performed by drawing tangents to the curve on both side of the breakpoints. For minor events, the reliability of the break points was ascertained by verifying that the OD vs. $[LIP]_{tot}$ of the mixed aggregates formed at these points verifies a Beer-Lambert law, in order to control that these aggregates have the same specific turbidity (28). The reproducibility of the experiments was controlled by four successive recordings of the solubilization of EPC/EPA REV ($[LIP]_{ini}$ = 0.5 mM) by addition of a 20 mM TC solution at 0.11 μmol/min. The errors on the determination of the $[TC]_o$ and R_e are 0.2mM and 0.02, respectively.

Resonance Energy Transfer Measurements

The insertion of TC into the lipid membrane was studied by incorporating lipid fluorescent probes (NBD-PE and Rhodamine-PE) in EPC/EPA REV according to the methodology developed by Paternostre *et al.* (22). The RET between the probes NBD-PE and Rho-PE describes the transfer of the energy accumulated by a donor (NBD-PE) to an acceptor (Rho-PE). It was measured by recording simultaneously the emission fluorescence intensity of NBD-PE (FI_{530}) at a wavelength (λ_{em}) of 530 nm and that of Rho-PE at a λ_{em} of 590 nm (FI_{590}), the sample being excited at 470 nm, the λ_{exc} of the donor. The solubilization profiles were then obtained by plotting the ratio (FI_{590}/ FI_{530}) between the fluorescence emission intensities of Rho-PE and NBD-PE vs. the total TC concentration.

The experiments were carried out on a spectrofluorimeter (Fluorolog Spex FL1T11, Jobin Yvon, Longumeau, France), connected to a computer. The solubilizations were performed at 25°C, in a quartz cell, under a constant stirring by using the procedure described for the continuous turbidity measurements. The initial vesicle dispersion was composed of a mixture of unlabeled and labeled EPC/EPA REV at a lipid molar ratio of 95/5 (M/M) to reduce as much as possible the inner filter effect. In these conditions, the fluorescence intensity ratio FI_{590}/ FI_{530} only depends on the TC insertion in the vesicle bilayers (22). A 20 mM TC solution was continuously added at a rate of 0.11 μmol/min to the vesicle dispersions with lipid concentrations ranging from 0.5 to 5 mM.

The efficiency of RET depends on the distance between both probes in the vesicle lipid bilayers. In the initial vesicles, this distance is sufficiently small to allow the RET to exist (FI_{590}/ FI_{530} maximum). Conversely, in the micelles, which are structures too small to integrate both types of probes in the same aggregate, the RET no longer occurs (FI_{590}/ FI_{530} minimum). It results that only the fluorescence of the donor (FI_{530}) is observed due to the dilution of the fluorescent lipids into numerous mixed aggregates very small in size. In the intermediate mixed aggregates, the insertion of surfactant molecules modifies the environment of the probes and decreases the RET. The RET is also influenced by the transfer of lipidic probes from labeled vesicles to unlabeled ones induced by the addition of detergent.

RESULTS

Phospholipid Bilayer Solubilization by TC

Figure 2a shows the variations of the turbidity of EPC SUV upon continuous addition of a 20 mM TC solution at a

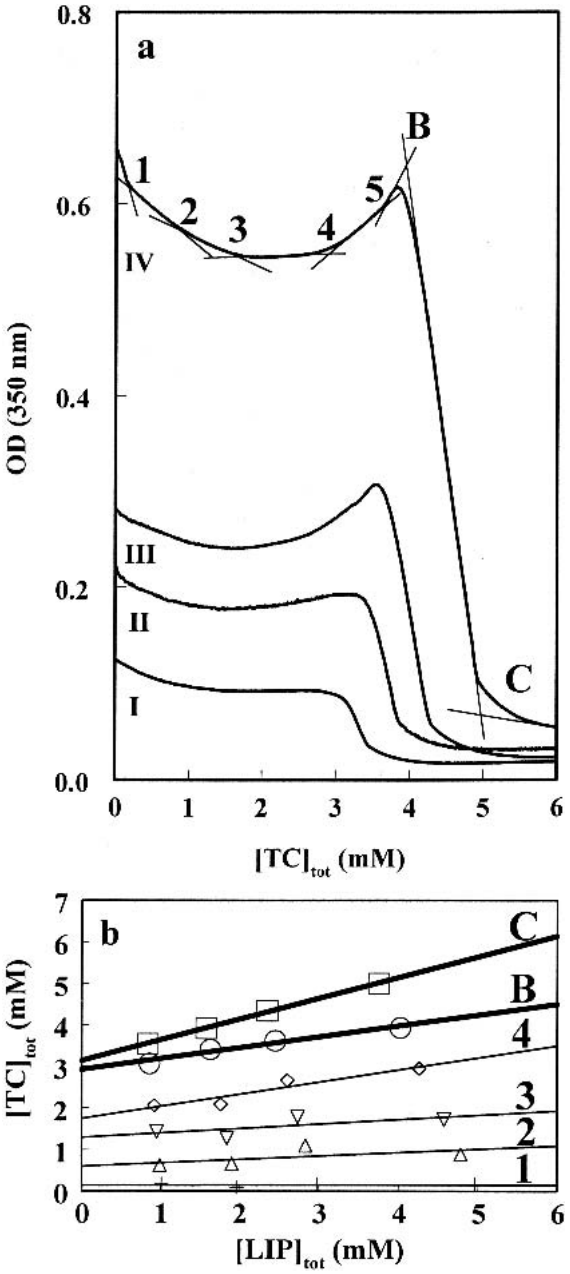

Fig. 2. Solubilization of EPC SUV by continuous addition of a 20 mM TC solution at 25°C. (a) Evolution of the turbidity (OD at 350 nm) vs. total surfactant concentration $[TC]_{tot}$:$[LIP]_{ini}$ (mM) = 1.02 (curve I), 1.97 (II), 3.00 (III), and 5.00 (IV). Rate of TC addition = 0.028 μmol/min. (b) Relationships between total TC concentration ($[TC]_{tot}$) and total lipid concentration ($[LIP]_{tot}$) determined at the characteristic points of the solubilization curves: Point 1 (+), point 2 (Δ), point 3 (∇), point 4 (◇), point B (○), and point C (□). The phase limits corresponding to points B and C are drawn in thick lines.

rate of 0.03 μmol/min to lipid vesicle dispersions of initial concentrations ranging from 1 to 5 mM. The profiles present a number of break points (noted 1 to 5 on curve IV, Fig. 2a) corresponding to minor variations of the OD curve in addition to sharp changes (B and C). The TC addition first leads to a gradual decrease in the turbidity of the initial vesicle dispersions until point 3, followed by an increase observed up to point B. Between B and C, OD strongly decreases in relation to the progressive formation of mixed TC/EPC micelles. Beyond point C, OD slowly decreases indicating morphology (size and/or shape) changes in the micelles by further addition of TC. With decreasing initial EPC concentration, the shape of the solubilization profiles is globally maintained. This shows that the same sequence of mixed intermediate aggregates (regarding their morphological characteristics) occurs upon addition of TC whatever the initial lipid concentration, except for point 5 which is only observed at the two highest lipid concentration analyzed.

The composition of the different mixed aggregates at the characteristic points (1 to 4, B and C) of the turbidity curves was determined by plotting the total TC concentration ($[TC]_{tot}$) vs. the total lipid concentration ($[LIP]_{tot}$) stated at these points (Fig. 2b). Using a linear regression analysis of the different plots, a linear relationship between $[TC]_{tot}$ and $[LIP]_{tot}$ was obtained for each point analyzed (Fig. 2b), according to the following equation (20,28):

$$[TC]_{tot} = [TC]_o + ([TC]/[LIP])_{ag} [LIP]_{tot} \quad (3)$$

where $[TC]_{tot}$ and $[LIP]_{tot}$ are the total TC and lipid concentrations, $[TC]_o$ is the concentration of TC molecules nonassociated with lipid (i.e., present in the aqueous phase), and $([TC]/[LIP])_{ag}$, also noted R_e, is the molar ratio of TC to lipid in the mixed aggregates. R_e is determined from the slope of the straight lines, and $[TC]_o$ is obtained by extrapolating $[LIP]_{tot}$ to zero. These parameters calculated by linear regression analysis are reported in Table I.

The linear relationships obtained for points 1 to 4 (Fig. 2b) indicate that the minor events observed on the turbidity profiles correspond, as for points B and C, to specific aggregate compositions in equilibrium with specific TC concentrations in the aqueous medium. Each straight line defines a specific aggregationnal state that has the same global composition whatever the lipid concentration. These aggregationnal states depict either successive steps in a monophase domain (vesicular domain) or phase limits with structure changes (micellization process).

Similarly to SUV, the solubilization of the large vesicles EPC/EPA REV was performed by a continuous addition of a 20 mM TC solution. The compositions of the characteristic intermediate mixed aggregates formed during the transition are presented in Table II. Points 1 to 4 (EPC SUV/TC) and 1 to 5 (EPC/EPA REV/TC) which reflect minor events are specific to each system, whereas B and C define the same phase limits for both systems. The TC concentration in the aqueous phase in equilibrium with the successive mixed aggregates (Tables I and II) was always lower than the TC CMC (6.5 mM, see "Materials and Methods") whatever the vesicle type.

Influence of the TC Addition Rate on the Solubilization Process

The effects of the addition rate of a 20 mM TC solution on the insertion of the surfactant molecules into the EPC SUV (Fig. 3a) and EPC/EPA REV (Fig. 3b) bilayers were studied at two rates of addition of 0.11 (curve I) and 0.03 μmol/min (curve II). The initial lipid concentration of the vesicle dispersions was varied from 1 to 5 mM. As an example, Figs. 3a and 3b display the OD profiles recorded for

Table I. Composition of Mixed Aggregates (R_e) and Concentration of Sodium Taurocholate (TC) in the Aqueous Medium ($[TC]_o$) at the Characteristic Points of the Turbidity Curves Recorded During the Solubilization of EPC SUV at 25°C by a Solution of 20 mM TC at Both Addition Rates

	Point 1		Point 2		Point 3		Point 4		Point B		Point 6		Point C	
Rate (μmol/min)	R_e	$[TC]_o$ (mM)	R_e	$[TC]_o$ (mM)	R_e	$[TC]_o$ (mM)	R_e	$[TC]_o$ (mM)	R_e	$[TC]_o$ (mM)	R_e	$[TC]_o$ (mM)	R_e	$[TC]_o$ (mM)
0.03	~0	0.1	0.08	0.6	0.11	1.3	0.29	1.8	0.26	2.9			0.50	3.1
0.11							0.07	1.9	0.31	3.0	0.46	3.0	0.50	4.5

EPC SUV, egg phosphatidylcholine small unilamellar vesicles.

the solubilizations of EPC SUV and EPC/EPA REV at $[LIP]_{ini}$ = 2 mM, respectively.

The evolution of the solubilization profiles of EPC SUV (Fig. 3a) and EPC/EPA REV (Fig. 3b) is clearly influenced by the addition rate of the detergent in the vesicular domain of the transition (i.e., up to point B). The continuous decrease in OD observed at the higher rate (0.11 μmol/min, curve I), is replaced by a more complex OD profile at the lower one (0.03 μmol/min, curve II). Between B and C, differences in the micellization process of EPC SUV by TC (Fig. 3a) are also evidenced. Indeed, the micelle formation takes place in two steps with the higher addition rate as indicated by the existence of the break point noted 6 (Fig. 3a, curve I) and observed whatever the lipid concentration (data not shown). The plots of $[TC]_{tot}$ vs. $[LIP]_{tot}$ related to points B, C for both systems and point 6 in the case of EPC SUV are reported in Figs. 3c and 3d. For the latter system, a strong influence of the addition rate on the intercept of the straight lines $[TC]_{tot}$ vs. $[LIP]_{tot}$ with y axis, is observed for point C (arrow). It is to note that the $[TC]_{tot}$ vs. $[LIP]_{tot}$ straight line corresponding to point 6, which is only observed at the higher rate, is very close to the straight line of point C obtained at the lower addition rate (Fig. 3c). The TC to lipid molar ratio in the aggregates (R_e) and the TC concentration in the aqueous medium $[TC]_o$ are summarized in Tables I and II for EPC SUV/TC and EPC/EPA REV/TC systems, respectively.

The influence of the addition rate of the TC solution on the vesicle-micelle transition of EPC/EPA REV was also studied with a TC solution twice less concentrated (9.95 mM instead of 20 mM) (Fig. 4, curves I to III). Vesicle dispersions with a fixed initial lipid composition ($[LIP]_{ini}$ = 0.978 mM) were solubilized by continuously adding the 9.95 mM TC solution at three addition rates (0.55 (curve I), 0.06 (curve II) and 0.03 (curve III) μmol/min). For the three recordings, a monotonic decrease in OD is observed down to a $[TC]_{tot}$ value close to 2 mM (Fig. 4). Up to this $[TC]_{tot}$, all profiles (I to III) are superimposed within experimental deviation. For 2 mM ≤ $[TC]_{tot}$ ≤ 3.25 mM, the solubilization profile is dependent on the addition rate. Lowering the addition rate induces changes in the supramolecular arrangements of the intermediate mixed aggregates as shown by the significant increase in turbidity (curves II and III). For all the rates studied, at $[TC]_{tot}$ > 3.25 mM, a quasi-linear decrease in OD is observed, with similar slopes for the two lowest rates (curves II and III) but a clearly less pronounced one for the highest rate (curve I). Then, the end of solubilization is marked by low turbidity values.

The solubilizations carried out at the addition rates of 0.03 and 0.55 μmol/min were performed in two successive steps (Fig. 4, curves I and III) because the cell volume did not allow containing of the surfactant volume required to achieve the solubilization process. Thus, an aliquot (about 1.5/2.5 v/v) of the sample obtained at the end of the first step was used to go on the solubilization by a further addition of the TC solution. The time pauses are indicated on curves I and III and delimited by vertical arrows. The experiment performed at 0.55 μmol/min was stopped at $[TC]_{tot}$ = 4 mM (curve I) for about 15 min. Upon further addition of TC ($[TC]_{tot}$ > 4 mM), OD regularly decreases, whereas the break point corresponding to point C is not detected. Nevertheless, OD values remain rather high although the mean diameter of the mixed lipid/TC dispersion obtained at the end of the second experiment was too small to be measured by QELS (∅ ~ <10 nm). Micellization would likely have partially occurred during the addition interruption. The solubilization performed at the addition rate of 0.03 μmol/min was stopped earlier at $[TC]_{tot}$ = 3.65 mM (Fig. 4 curve III) and then carried on after waiting 12 h. The mean diameter of the mixed aggregates was measured just before resuming the experiment. A mean diameter of 149 ± 7 nm was found from unimodal analysis. The SDP intensity analysis indicates besides a population of 148.6 ± 7.5 nm, a minor fraction (6%) of very small particles (10 nm). This

Table II. Composition of Mixed Aggregates (R_e) and Concentration of Sodium Taurocholate (TC) in the Aqueous Medium ($[TC]_o$) at the Characteristic Points of the Turbidity Curves Recorded During the Solubilization of EPC/EPA REV Unlabeled or Labeled (*) with NBD-PE and Rhodamine-PE at 25°C by a Solution of 20 mM TC at Both Addition Rates

	Point 1		Point 2		Point 3		Point 4		Point 5		Point B		Point C	
Rate (μmol/min)	R_e	$[TC]_o$ (mM)	R_e	$[TC]_o$ (mM)	R_e	$[TC]_o$ (mM)	R_e	$[TC]_o$ (mM)	R_e	$[TC]_o$ (mM)	R_e	$[TC]_o$ (mM)	R_e	$[TC]_o$ (mM)
0.03							0.07	2.0			0.20	2.4	0.51	3.3
0.11											0.15	2.9	0.40	3.4
0.11*	~0	0.3	~0	0.9	0.04	1.4	0.15	2.0	0.23	2.3	0.27	2.9	0.58	3.3

EPC/EPA REV, egg phosphatidylcholine/egg phosphatidic acid large unilamelar vesicles.

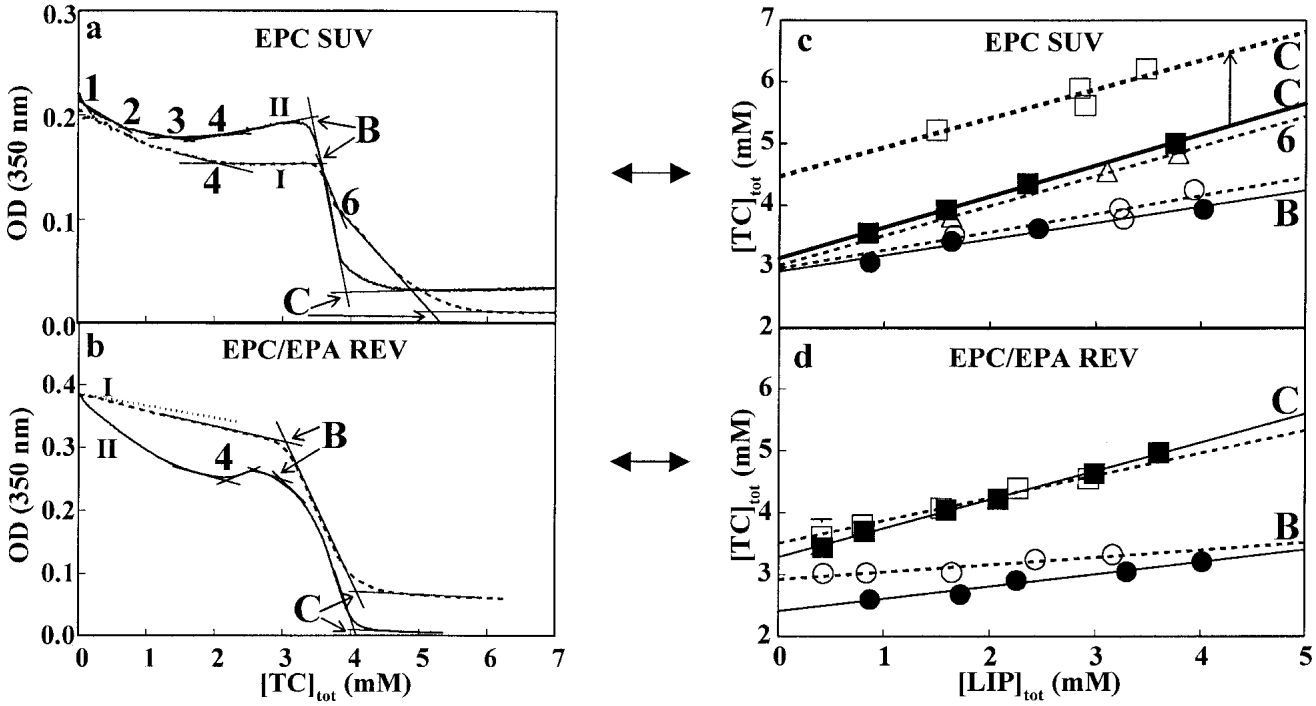

Fig. 3. Influence of the addition rate of a 20 mM TC solution on the turbidity curves recorded at 350 nm and 25°C and on the characteristic straight lines obtained along the solubilization process of (a, c) EPC SUV and (b, d) EPC/EPA REV. (a, b) $[LIP]_{ini}$ = 2 mM; rate of TC addition = 0.11 (curve I,----) and 0.03 (curve II, —) μmol/min. (b) The dotted line shows the calculated decrease of OD induced by simple vesicle dilution. (c, d) Rates of TC addition = 0.11 μmol/min (dashed lines): point B (○), point 6 (Δ) and point C (□); 0.03 μmol/min (full lines): point B (●) and point C (■).

result shows that likely the dispersion still contained vesicular mixed aggregates in coexistence with mixed micelles after 12 h of pause. As the scattering of micelles is very weak compared to that of large particles, the proportion of both particle populations cannot be determined. Upon further addition of the TC solution (curve III beyond the arrow), point C specific of the solubilization end occurs for a total TC concentration of 3.91 mM. The drops in OD observed during the solubilization interruption are mainly due to a time evolution of the sample turbidity as shown by the decreases observed at the three addition rates (Fig. 4 inset).

Influence of the Concentration of the Initial TC Solution on the Solubilization Process

To check the role of the aggregation state of TC in the initial solution, we have reported on Fig. 4 (curve IV) the solubilization profile obtained with an EPC/EPA REV dispersion ([LIP] = 1 mM) by addition of a 20 mM TC solution instead of the 9.95 mM TC solution. Curves III and IV corresponding to the addition of the 9.95 and 20 mM TC solution, respectively at the same slow rate of 0.03 μmol/min show that the similar shape of the solubilization profile is obtained except that the supramolecular rearrangements observed in the vesicular domain occur earlier with the diluted TC solution. In fact, in this domain curve IV is superimposed to curve II, that is, adding a 9.95 mM TC solution at 0.03 μmol/min or a 20 mM TC solution at 0.06 μmol/min leads to the same supramolecular organization for the mixed aggregates. As already shown (21), the solubilization of liposomes essentially results in interactions of the surfactant with lipid aggregates independently of the initial aggregation state of the surfactant. With both initial TC concentrations used in this work, the surfactant dilution in the aqueous continuum of the vesicle suspension, leads almost instantaneously to concentrations lower than the CMC of the surfactant (6.5 mM, see "Materials and Methods"), as the transition of the vesicles into mixed micelles is achieved at a total TC concentration added lower than 6 mM (Figs. 2 and 3). Then, it may be reasonably considered that TC predominantly interacts with the lipid as monomers.

Continuous turbidity recordings show that the solubization mechanism of vesicles by TC is governed by complex kinetics. Reducing the addition rate of TC leads to morphological rearrangements of the mixed TC/Lip aggregates in the vesicular domain, as shown by the changes in the OD profiles (Figs. 3 and 4). The kinetic effect is more pronounced for EPC/EPA REV, as the occurrence of additional breakpoints on the solubilization profiles (Fig. 3b, curve II and 4, curves II to IV) clearly indicates that new supramolecular arrangements of specific composition can be formed by lowering the addition rate. Conversely, the linear decrease characterizing the beginning of the OD profile recorded at the faster rate (0.11 μmol/min) for EPC/EPA REV (Fig. 3b, curve I) is very close to the line which would have been observed upon simple vesicle dilution, (Fig. 3b, doted line). This suggests that when TC is rapidly added to the vesicle dispersion, the interaction of TC molecules with the external bilayer of the vesicles is strongly limited in the first step of the vesicle-micelle transition. It results that the partitioning of TC in the vesicular domain is governed by the addition rate of TC (Tables I and II). When the vesicles are saturated with TC at B and at the end of the micellization at C, this effect is apparently reduced,

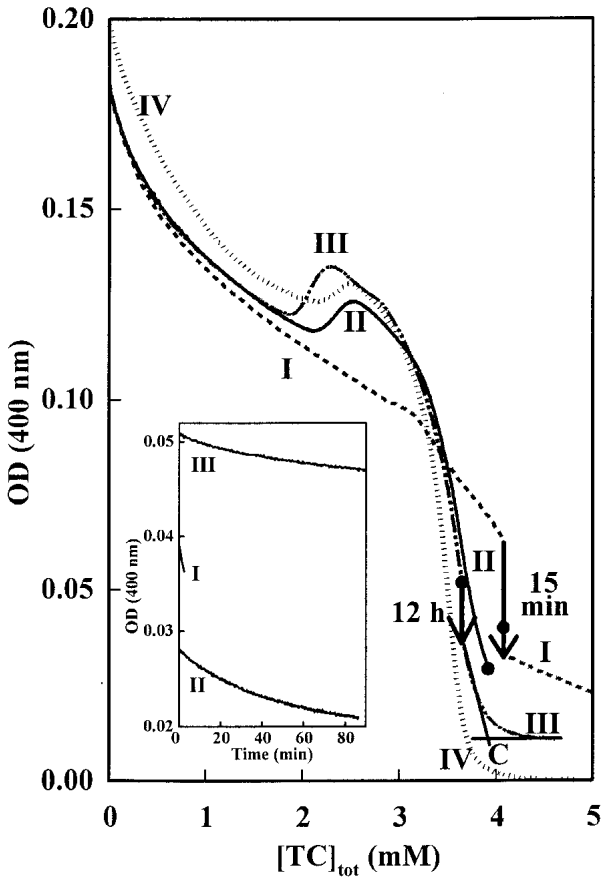

Fig. 4. Influence of the addition rate of TC on the solubilization of EPC/EPA REV at 25°C. $[LIP]_{ini}$ = 0.978 mM, addition rate of a 9.95 mM TC solution = 0.55 (curve I, ----), 0.06 (curve II, —) and 0.03 μmol/min (curve III, — - - —). Curves I and III were recorded in two steps (see "Results"). The vertical arrows on curves I and III indicate the drop of OD occurring during the pause of TC addition. The evolutions of OD vs. time during this interruption are reported in the inset. They were measured either just at the stop (curves II and III) or just before the second step (curve I), as indicated by full squares on the main figure. The recordings were started again after a time of 15 min and 12 h for curves I and III, respectively. Curve IV represents the recording at 25°C of the solubilization of EPC/EPA REV ($[LIP]_{ini}$ = 1 mM) by addition of a 20 mM TC solution at 0.03 μmol/min. OD was measured at 400 nm.

as the respective compositions (R_e) of the mixed aggregates are almost insensitive to the addition rate. However, for EPC SUV, if increasing the addition rate of TC does not change the amount of TC molecules inserted in the mixed micelles formed at point C (R_e = 0.5), TC molecules significantly accumulate in the external aqueous continuum of the SUV from 3.1 to 4.5 mM (Table I; Fig. 3c). Beyond point B, a kinetic limitation is also observed during the micellization process of SUV with the faster addition rate of TC. At the intermediate step corresponding to point 6, the composition of the aggregates and the TC concentration in the aqueous phase (R_e = 0.46, $[TC]_o$ = 3.01 mM) are very close to that of the mixed micelles (point C, Fig. 3a, curve II) formed with the slower rate of addition (R_e = 0.50, $[TC]_o$ = 3.1 mM) (Table I). It should be noted that the morphology (number, shape, and/or size) of the aggregates formed in these both conditions are quite different despite their similar compositions, as the OD value of point 6 is about three times higher. This suggests the persistence of lamellar fragments or large mixed particles, likely due to a heterogeneous distribution of the bile salt in the lipidic structures when TC is rapidly added (Fig. 3a, curve I). The second part of the micellization process between point 6 and C reflects a progressive reorganization of these aggregates into small mixed micelles without changing the global TC/Lip molar ratio associated to these structures. This evolution toward smaller objects indicates that diffusion of the TC molecules in the lipid matrix requires time. Lowering the addition rate of the surfactant favors a homogeneous distribution of the TC molecules in the aggregates so that the intermediate stage described above no longer occurs in the micellization process.

Fluorescence Measurements

Figure 5a shows the evolution of the fluorescence intensity ratio FI_{590}/FI_{530} vs. the TC concentration for four different initial lipid concentrations (1, 2, 3, and 4 mM) at the TC addition rate of 0.11 μmol/min. In parallel, the solubilization of the same vesicle populations was followed by turbidity (Fig. 5b) with the same rate of TC addition so that the composition of the successive aggregates formed during the solubilization process remained identical for both analyses. As previously observed, the turbidity profiles obtained with increasing lipid concentration are homothetic, allowing determination of the composition of the mixed aggregates at different specific points of the curves (1 to 5, B and C, Table II).

At the onset of the TC addition in the vesicles, the fluorescence intensity ratio FI_{590}/FI_{530} decreases slowly and linearly down to the point noted F corresponding to the threshold of the deviation from linearity. At this point, a linear relation between $[TC]_{tot}$ and $[LIP]_{tot}$ is obtained. Values of 1.3 mM and 0.05 were found for $[TC]_o$ and R_e, respectively, which are very close to the composition of the mixed aggregate related to point 3 ($[TC]_o$ = 1.4 mM, R_e = 0.04) determined from OD recordings (Fig. 5c). Beyond point F, the decrease in RET becomes more pronounced and suggests an increasing insertion of TC molecules within the phospholipid bilayers (Fig. 5a). Finally the fluorescence intensity ratio FI_{590}/FI_{530} tends to a plateau of very low values due to the disappearance of the RET in relation to the existence of mixed micelles. The break point noted G (Fig. 5a) represents a phase limit beyond which RET no longer occurs. A linear relation between $[TC]_{tot}$ and $[LIP]_{tot}$ is also observed for this point (Fig. 5c). It is worth noting that very close values of R_e are found for point G (0.59) determined from RET measurements and point C (0.58) obtained from OD recordings, indicating that mixed micelles of the same composition are formed at C and G. However, the concentration of TC in the aqueous phase $[TC]_o$ is higher for G (3.8 mM) than for C (3.3 mM) (Fig. 5c).

DISCUSSION

The continuous turbidity experiments allows to determine the partition of the surfactant in the lipid aggregates, which gives the TC insertion efficiency at specific steps of the solubilization process. The insertion efficiency is depicted by the evolution of the molar fraction of TC in the aggregates $[R_e/(R_e + 1)]$ vs. the TC concentration in the aqueous medium

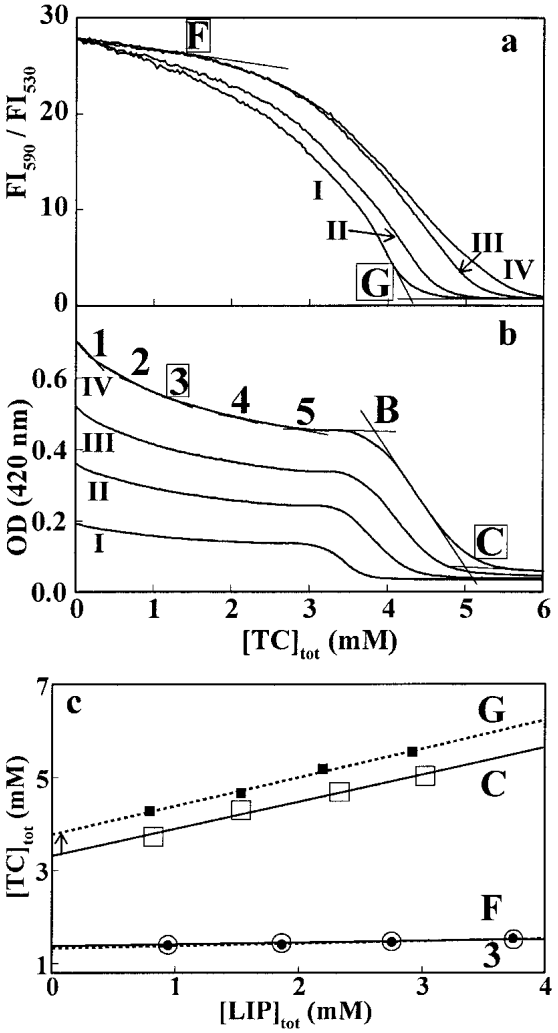

Fig. 5. Insertion of TC into EPC/EPA REV labeled with NBD-PE and rhodamine-PE during the solubilization process by a 20 mM TC solution added at 0.11 μmol/min at 25°C. Evolution of (a) the ratio of fluorescence emission intensities at 590 and 530 nm (FI_{590}/FI_{530}) and (b) the turbidity (420 nm) vs. total TC concentration $[TC]_{tot}$. $[LIP]_{ini}$ (mM) = 1.02 (curve I), 2.01 (II), 2.97 (III), and 4.06 (IV). (c) Relationships between total TC concentration ($[TC]_{tot}$) and total lipid concentration ($[LIP]_{tot}$) at characteristic points F (●), G (■), 3 (○) and C (□) determined from the RET (full symbols) and OD (empty symbols) curves, respectively.

($[TC]_o$) (29,22). This evolution provides information on the interaction mode of TC with the lipid membrane and the degrees of its insertion in the bilayer as TC addition goes along, which enlighten the mechanisms of the progressive conversion of vesicles into mixed micelles.

Equilibrium State of Taurocholate/Lipid Mixed Aggregates

The slow process of TC distribution within the lipidic structures may result in the formation of mixed aggregates out of equilibrium during the vesicle-micelle transition. The supramolecular rearrangements observed in the vesicular domain (Figs. 3 and 4) when the addition rate of TC is slowed down shows that obtaining mixed aggregates in an equilibrium state would require use of extremely low addition rates of TC. The micellization process also evidences metastable mixed aggregates. Indeed the slowness of the homogeneous distribution of TC molecules within the lipid membrane delays the transformation into small mixed micelles when TC is added at a high rate (Figs. 3a and 3c). This is also evidenced by the evolution of the turbidity observed during the interruption of the TC addition to EPC/EPA REV (Fig. 4, curves I and III). With the slowest TC addition used (0.03 μmol/min), the vesicle transition into mixed micelles is achieved at a total TC concentration ($[TC]_{tot}$) of 3.91 mM (Fig. 4, curve III, point C). It results that $[TC]_{tot}$ (4.08 mM) at which curve I recorded at the highest rate (0.55 μmol/min) was stopped, slightly exceeds the effective TC amount necessary to solubilize the vesicles, whereas the high OD value (0.0630) shows that in this case, the transition is just in progress. However, the sharp drop of OD vs. time (Fig. 4 inset, curve I) in conjunction with the nondetection of point C and the existence of particles too small in size to be measured by QELS at the end of the second addition step suggest that micellization may have occurred during the pause of TC addition for 15 min. Equilibrium state is obviously favored by reducing the rate of TC addition as seen from the solubilization recorded at the slowest rate (Fig. 4, curve III). Indeed, the system at the end of the first part evolves only slightly as the global decrease of OD vs. time remains low after 12h (Fig. 4 inset, curve III). Moreover, at the time of stopping the TC addition, the micellization process is more advanced than in case of curve I as the OD value is lower. This transition level is obtained with a lower amount of TC (3.65 mM), so that a slow addition of the surfactant favors its homogeneous distribution within the lipid membrane and helps the micellization to progress under conditions closer to equilibrium. A true equilibrium state would however require to slow down still more the rate of TC addition as indicated by the OD variation observed vs. time, even if this one is rather weak.

These results show that very slow processes kinetically govern the formation of lipid-TC supramolecular arrangements in an equilibrium state. Nevertheless, analysis in a continuous way of mixed TC/lipid aggregates out of equilibrium is of interest to approach the dynamic aspects observed in digestion or drug delivery. From this point of view, it is particularly interesting that in the vesicular domain, the vesicle architecture remains intact when TC is added at a high rate as shown by the OD variation similar to that which would be obtained upon simple vesicle dilution (Fig. 3b).

Mechanisms of TC Interaction and Insertion in the Phospholipid Membrane

The partitioning of TC in the lipid aggregates obtained for labeled EPC/EPA REV and EPC SUV at the fastest rate of the TC addition studied in this paper (0.11 μmol/min) is reported in Fig. 6 as a dynamic approach to the action of bile salts in the digestion phenomena. The surfactant partitioning is changing along the vesicle-micelle transition. Three domains can be delimited, two in the vesicular part and one in the micellar part of the solubilization process.

Vesicular Domain: A Two-Step Insertion Mechanism

Figure 6 shows that the first stage of the solubilization process is characterized by the absence of TC insertion in the bilayers. The upper limit of the domain of noninsertion of the

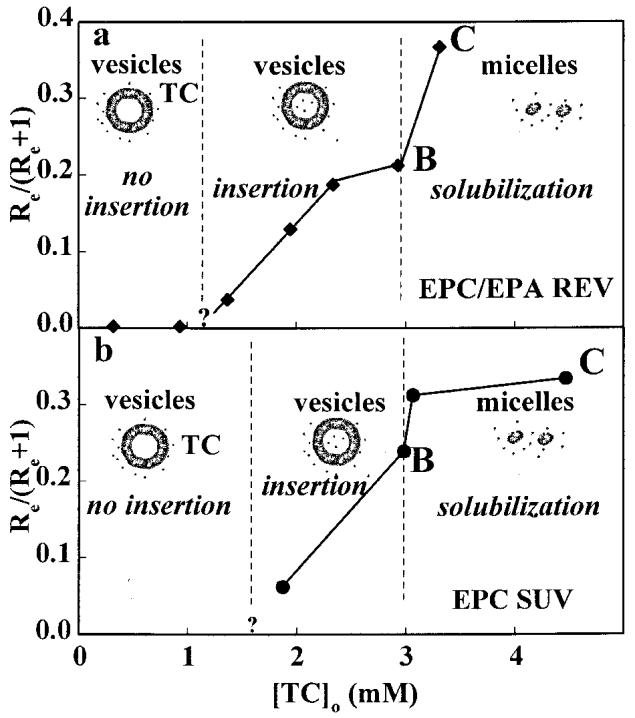

Fig. 6. Comparison of the insertion of TC in (a) EPC/EPA REV labeled with NBD/Rho and (b) EPC SUV at the addition rate of TC = 0.11 μmol/min and 25°C. The partition coefficient of TC between the aggregates and the aqueous medium is represented by the evolution of the molar fraction of TC in the aggregates ($R_e/(R_e+1)$) vs. the concentration of TC in the aqueous medium ($[TC]_o$). The TC/EPC molar ratio in the aggregates (R_e) and $[TC]_o$ were deduced from the respective slopes and origins of the different straight lines obtained for each specific point as reported in Tables I and II.

surfactant may be approximately located around $[TC]_o$ values of 1.2 mM for EPC/EPA REV and 1.6 mM for EPC SUV, respectively (Fig. 6, dashed vertical lines) with the fast rate of TC addition. However, for the latter vesicles, this domain is more restricted when the rate of TC addition is reduced since the threshold of TC insertion can be estimated occurring for $0.1 < [TC]_o < 0.6$ mM (between points 1 and 2, Table I). The second step of the solubilization (Fig. 6) is insertion of the surfactant into the vesicles. The question arises whether the thresholds of insertion measurable by the continuous turbidity recordings correspond to incorporation of the surfactant into the external and internal leaflets of the bilayer. Permeabilization of EPC/EPA REV by TC was followed with the same strategy of TC addition as here (30,31). The leakage of a fluorescent dextran (fluorescein isothiocyanate (FITC)-dextran of 4400 molecular mass) was measured after stopping the surfactant addition at successive amounts of TC according to a methodology that maintains the surfactant partitioning between the lipid bilayer and the aqueous medium (30). The onset of the probe release, which proves insertion of the bile salt in both monolayers of the vesicles, was observed for a $[TC]_o$ value of 1.64 mM, that is, a TC concentration in the aqueous medium slightly higher than that at which a molar fraction of TC in the lipid bilayer can be measured by turbidity (Fig. 6a). This result strongly suggests that the threshold obtained from our turbidity experiments corresponds to the onset of the incorporation of the TC molecules within the hydrophobic interior of the lipid bilayers.

The interactions of bile salts with phospholipids are essentially governed by the polar and apolar properties of these molecules. Taurocholate is a roughly planar molecule with a polar face made up of three hydroxyl and one taurine groups and a nonpolar face made up of the hydrocarbon elements of the steroid. EPC consists of a hydrophilic phosphorylcholine head group and a hydrophobic tail composed of a mixture of saturated and unsaturated hydrocarbon chains.

In the first stage of the solubilization process, the planar geometry and the hydrophilic face of bile salt may explain the non-insertion of TC molecules within the lipid bilayer observed from our turbidity experiments. It, therefore, may be assumed that the TC molecules as monomers are located in the headgroups of the lipids at the water interface with the polar face directed toward the external water medium and the hydrophobic part oriented toward the lipid chain without interacting with them, as observed previously with another molecule containing a polar face and a hydrophobic one (32). Such a molecular organization might be the cause of the very small decrease in the fluorescence intensity ratio FI_{590}/FI_{530} observed in this part of the vesicle to micelle transition for EPC/EPA REV (Fig. 5a), which suggests that the lipid membrane is only slightly affected by the TC molecules. This result can be directly compared to the partitioning of octyl β-D-glucopyranoside (OG) studied by Paternostre and co-workers (22) as we used the same vesicular system and experimental conditions as these authors. In the case of OG, which is a non-ionic surfactant with a short saturated straight acyl chain, the first part of the solubilization is characterized by a continuous variation of the partition coefficient, which induces a net RET decrease.

Localization of TC molecules in the polar head groups of the outer leaflet of EPC vesicles at low TC concentrations has been proposed by Walde *et al.* (33) on the basis of fluorescence measurements using bromothymol blue and 1,6-diphenyl–1,3,5-hexatriene (DPH) as surface and hydrophobic probes, respectively. X-ray diffraction experiments performed on multilamellar dipalmitoylphosphatidylcholine (DPPC)-TC mixtures have evidenced a drastic increase in the repeat distance of the DPPC lamellar structure due to electrostatic repulsion between bilayers, at low TC/DPPC molar ratios corresponding to the TC noninsertion domain observed in the current study (31). Studies of the interactions of sodium cholate with EPC membranes have led to similar conclusions at low cholate/lecithin molar ratios. From equilibrium binding measurements, Schubert and co-workers (14) have proposed that cholate binds to the external monolayer of EPC vesicles, the cholate molecules being adsorbed on the membrane surface with a maximum binding of six lecithin molecules per one cholate molecule. At this cholate concentration the vesicles remained impermeable to a raffinose carbohydrate of low molecular mass.

In the insertion domain, incorporation of the bile salt in both monolayers of the lipid membrane implies a molecular rearrangement of the surfactant molecules into dimeric structures by assembling their hydrophilic sides in order to expose their hydrophobic moiety to the lipid hydrocarbon chains. The TC dimeric aggregates are therefore inserted perpendicular to the membrane surface. Such a dimeric organization in lecithin bilayer membrane has been found with specifically deuterated deoxycholate and chenodeoxycholate (34).

For EPC/EPA REV, which are monodisperse unilamel-

lar vesicles, the linear region in the partition coefficient (Fig. 6a) would indicate the existence of a biphasic domain, that is, a TC-rich lamellar phase and an aqueous phase. Indeed, a linear law is characteristic of a two-phase domain, the structural properties of the two phases remaining unaffected by increasing the concentration of the external molecule partitioning between them. (22). The TC partitioning decreases at the end of the insertion domain probably due to the saturation of the membrane interior by bile salt dimers. For EPC SUV which are an aggregated population of unilamellar vesicles, the information available from the turbidity data (Fig. 6b) indicates that the same TC partitioning as for EPC/EPA REV is obtained at the end of the insertion domain (Fig. 6 points B).

Micellar Domain: Existence of a Slow Process of Micelle Formation

The progressive transformation of the surfactant-saturated lamellar structures into mixed micelles between B and C is characterized by an increase in the partition coefficient of TC in the lipids (Fig. 6). During the micellization process TC partitions between mixed lamellar and mixed micellar aggregates and water. The composition of the mixed surfactant/lipid micelles formed through the micellization process at C is defined by a TC/Lipid molar ratio (R_e = 0.5 to 0.6) in the membrane globally twice that of the mixed aggregates at B (Tables I and II). One TC per two EPC molecules solubilizes the lipid membrane. The bile salt enrichment of the lipid bilayer beyond point B causes the rupture of the membrane into mixed TC dimers/lipid lamellar fragments of either disk (8,35) or rod-like (12,36) shapes. More recently, a time-resolved study by light and small-angle neutron scattering (18) of the evolution of the aggregate structures involved in the transformation of micelles into vesicles has demonstrated that upon dilution the shape of the relatively monodisperse spherical micelles changes to elongated, flexible, and locally cylindrical polymeric structures. The locally cylindrical micelles very quickly change their morphology to disks, which then transform into closed unilamellar vesicles in a slow process. Variations of the OD level observed in the micellar domain (Fig. 3) suggest formation of nonequilibrium micellar aggregates, the size and shape of which are sensitive to the rate of TC addition. Micellar structural reorganization is also illustrated by the RET measurements performed on the EPC/EPA REV-TC system. At the end of the micellization process determined by OD (i.e., at point C), a residual RET is still observed, which vanishes upon further TC addition at point G (Fig. 5). This observation leads to suppose the formation of large mixed micelles at point C in which the distance between donor and acceptor probes still enables a weak energy transfer to occur. The fact that the turbidity of the mixed micelles is lowered when the RET is removed at point G suggests that the large micelles evolve into a number of small ones with the probes distributed among distinct aggregates. The relative composition in lipid and surfactant of the mixed micelles at C and G (R_e = 0.58 and 0.59, respectively) remains unchanged during the reorganization process of the micellar aggregates, whereas the TC concentration in the aqueous medium is varying (from 3.3 to 3.8 mM; Fig. 5C). Lateral diffusion of the bile salt molecules and redistribution of the probes into the mixed micelles would be governed by a slow kinetic that delays the disappearance of the RET. A similar micellar reorganization from large aggregates into small ones at constant TC/lipid composition in the particles is also observed during the two-step micellization process observed with EPC SUV when TC is added rapidly (Fig. 3a, curve I)

The aqueous TC concentration in equilibrium with the mixed aggregates at each break point is well below the pure surfactant CMC, as generally observed in binary systems of pure EPC with various surfactants (cholate, octyl glucoside) (Tables I and II) (10,20). This behavior is also verified under our experimental conditions when the slow diffusion of the TC molecules within the lipid membrane causes surfactant accumulation in the aqueous medium. As the solubility of phospholipid in water is very low, the aqueous TC concentration in equilibrium ($[TC]_{oC}$) with the mixed micelles at point C assuming ideal mixing within the micelle (37), can be calculated by

$$[TC]_{oC} = [R_e/(R_e + 1)]_C \times CMC_{TC} \quad (4)$$

where $[(R_e/(R_e + 1)]_C$ is the mole fraction of the surfactant in the micelle at point C and CMC_{TC} is the micellar concentration of the pure surfactant. This evaluation gives 2.2 and 2.4 mM for $[TC]_{oC}$ in the case of EPC SUV and EPC/EPA REV, respectively, at the fastest rate of TC addition, compared to the respective experimental values of 4.5 and 3.3 mM (Tables I and II). The same trend is seen when TC is added more slowly. The divergence observed might also reflect the slow process of TC distribution within the mixed micelles leading to accumulation of TC molecules in the aqueous medium in excess. Another hypothesis could be a non-ideal mixing behavior.

Comparison of the solubilizing power of sodium taurocholate (this work) and cholate (10) toward the same vesicle type (EPC/EPA REV) results in a slight enhancement of the capacity of the taurine derivative to disrupt the lipid membrane. Indeed, micellization at point C is achieved for a cholate/ lipid molar ratio of 0.9 instead of a TC/lipid molar ratio of 0.6. An effect of the same order between the two bile salts was observed for the solubilization of large unilamellar vesicles obtained by controlled dialysis (38). The hydrophilic taurine group increases the polar surface of the bile salt, which might explain the relatively lower amount of TC necessary to transform lamellar structures into micellar ones.

CONCLUSIONS

The choice of a continuous light scattering technique allows precise description of the successive stages of the vesicle to micelle transition and to evidence kinetically controlled phenomena. A very interesting aspect of such a methodology is to obtain the composition of different intermediate surfactant/lipid aggregates either in an equilibrium state or not, encountered along the solubilization process. It also provides information concerning kinetics as well as existence and evolution of nonequilibrium or metastable states. This constitutes a dynamic approach in the study of interactions of TC with phospholipid membranes in view of understanding the physicochemical processes that may occur under physiological conditions.

The solubilization mechanism of lipids by TC is governed by complex kinetics, which depend on the surfactant concentration and its addition rate. A two-step process, that is, ad-

sorption of TC molecules at the external membrane surface followed by their insertion within the vesicle bilayers, characterizes the evolution of the vesicular state before its complete breakdown into mixed micelles. The destabilization process of the vesicle bilayers is very slow. Even after membrane solubilization, the micellar aggregates require a long time to equilibrate. As a whole, the major stages of the vesicle-micelle transition occurs at constant specific TC to lipid molar ratios in the mixed aggregates independently of the addition rate of TC, in contrast to the TC concentration in the aqueous phase, which is increasing with increasing addition rate. At the insertion threshold when TC molecules can no longer be adsorbed on the external surface of the vesicles, TC reorganizes into dimeric aggregates. This process is slow as well as the subsequent penetration and homogeneous distribution of the dimeric structures within the lipid membrane. The slow kinetics of vesicle solubilization presumably come from the polar/apolar properties of bile salts and phospholipids, that is, the polar/apolar surface of the surfactant molecule in opposite to the hydrophilic moiety located at one extremity of the long hydrophobic chain of the phospholipids.

In biological processes of digestion, the impact of TC on liposomes will depend on the concentration and flow rate of bile salt during the gastrointestinal tract. At low TC concentration [as in the intestinal lumen under fasted conditions (39)], a fast circulation rate of TC will maintain intact the vesicular architecture. This has interesting implications for oral delivery via liposomes. Under high level of bile salts such as postprandially or after lipid absorption, the lipid bilayer destructuration will be a function of the duration of contact between lipids and bile salts.

The methodology used in this work may be applied to quantify the composition of mixed lipid/surfactant aggregates formed with other bile salts constituting the natural bile either separately or in mixtures to obtain a better understanding of their interaction mode with lipids, which is of importance regarding the fate of liposomes *in vivo*. From a general viewpoint, continuous turbidity measurements offer an interesting route to get precise description of the impact of host molecules with colloidal vehicles like liposomes and emulsions.

ACKNOWLEDGMENTS

This work was supported by grants from MENESR and IFSBM. We thank Marie-Martine Boissonade and Dr. Adam Baszkin for their help in the determination of the critical micellar concentration of the sodium taurocholate.

REFERENCES

1. J. Dufourcq. Physico-chimie des phospholipides. In F. Puisieux (ed.), *Les liposomes: applications thérapeutiques,* Lavoisier, Paris, 1985, pp. 1–40.
2. M. Wacker and R. Schubert. From mixed micelles to liposomes: critical steps during detergent removal by membrane dialysis. *Int. J. Pharm.* **162**:171–175 (1998).
3. D. J. Cabral and D. M. Small. Physical chemistry of bile. In S. G. Schultz, J. G. Forte and B. B. Rauner (eds.), *Handbook of Physiology. The Gastrointestinal System, Section 6, Volume III*, Oxford University Press, New York, 1989, pp. 621–662.
4. D. Lichtenberg. Liposomes as a model for solubilization and reconstitution of membranes. In Y. Barenholz and D.D. Lasic (eds.), *Handbook of Nonmedical Applications of Liposomes*, CRC Press, Boca Raton, 1996, pp. 199–218.
5. W. J. Xia and H. Onyuksel. Mechanistic studies on surfactant-induced membrane permeability enhancement. *Pharm. Res.* **17**: 612–618 (2000).
6. J. Guo, Q. Ping, G. Sun, and C. Jiao. Lecithin vesicular carriers for transdermal delivery of cyclosporin A. *Int. J. Pharm.* **194**:201–207 (2000).
7. M. Ollivon, S. Lesieur, C. Grabielle-Madelmont, and M. Paternostre. Vesicle reconstitution from lipid-detergent mixed micelles. *Biochim. Biophys. Acta* **1508**:34–50 (2000).
8. N. A. Mazer. G.B Benedek, and M.C. Carey. Quasielastic light scattering studies of aqueous biliary lipid systems. *Biochemistry* **67**:601–615 (1980).
9. P. Schurtenberger, N. Mazer, S. Waldvogel, and W. Känzig. Preparation of monodisperse vesicles with variable size by dilution of mixed micellar solutions of bile salts and phosphatidylcholine. *Biochim. Biophys. Acta* **775**:111–114 (1984).
10. M.-T. Paternostre, M. Roux, and J. L. Rigaud. Mechanisms of membrane protein insertion into liposomes during reconstitution procedures involving the use of detergents. *Biochemistry* **27**: 2668–2677 (1988).
11. A. S. Luk, E. W. Kaler, and S. P. Lee. Structural mechanisms of bile salt-induced growth of small unilamellar cholesterol-lecithin vesicles. *Biochemistry* **36**:5633–5644 (1997).
12. A. Walter, P. K. Vinson, A. Kaplum, and Y. Talmon. Intermediate structures in the cholate- phosphatidylcholine vesicle-micelle transition. *Biophys. J.* **60**:1315–1325 (1991).
13. S. Almog, T. Kushnir, S. Nir, and D. Lichtenberg. Kinetic and structured aspects of reconstitution of phosphatidylcholine vesicles by dilution of phosphatidylcholine-soduim cholate mixed micelles. *Biochemistry* **25**:2597–2605 (1986).
14. R. Schubert, K. Beyer, H. Wolburg, and K. H. Schmidt. Structural changes in membranes of large unilamellar vesicles after binding of sodium cholate. *Biochemistry* **25**:5263–5269 (1986).
15. K. Andrieux, L. Forte, G. Keller, C. Grabielle-Madelmont, S. Lesieur, M. Paternostre, C. Bourgaux, P. Lesieur, and M. Ollivon. Study of DPPC/TC/water phase diagram by coupling of synchroton SAXS and DSC: I Equilibration kinetics. *Progress Colloid Polymer Sci.* **110**:280–284 (1998).
16. L. Forte, K. Andrieux, G. Keller, C. Grabielle-Madelmont, S. Lesieur, M. Paternostre, C. Bourgaux, P. Lesieur, and M. Ollivon. Sodium taurocholate-induced lamellar-micellar phase transitions of DPPC determined by DSC and X-ray diffraction. *J. Therm. Anal.* **51**:773–782 (1998).
17. C. H. Spink, V. Lieto, E. Mereand, and C. Pruden. Micelle-vesicle transition in phospholipid-bile-salt mixtures. A study by precision scanning calorimetry. *Biochemistry* **30**:5104–5112 (1991).
18. S. U. Egelhaaf and P. Schurtenberger. Micelle-to-vesicle transition: a time-resolved structural study. *Phys. Rev. Lett.* **82**:2804–2807 (1999).
19. J. Lasch. Interaction of detergents with lipid vesicles. *Biochim. Biophys. Acta* **1241**:269–292 (1995).
20. M. Ollivon, O. Eidelman, R. Blumenthal, and A. Walter. Micelle-vesicle transition of egg phosphatidylcholine and octyl glucoside. *Biochemistry* **27**:1695–1703 (1988).
21. G. A. Ramaldes, E. Fattal, F. Puisieux, and M. Ollivon. Solubilization kinetics of phospholipid vesicles by sodium taurocholate. *Colloids and Surfaces B* **6**:363–371 (1996).
22. M.-T. Paternostre, O. Meyer, C. Grabielle-Madelmont, S. Lesieur, M. Ghanam, and M. Ollivon. Partition coefficient of a surfactant between aggretates and solution: Application to the micelle-vesicle transition of egg phosphatidylcholine and octyl β-D-glucopyranoside. *Biophys. J.* **69**:2476–2488 (1995).
23. A. D. Bangham, M. M. Standish, and J. C. Watkins. Diffusion of univalent ions across the lamellae of swollen phospholipids. *J. Mol. Biol.* **13**:238–252 (1965).
24. S. Lesieur, C. Grabielle-Madelmont, M.-T. Paternostre, and M. Ollivon. Size analysis and stability study of lipid vesicles by high-performance gel exclusion chromatography turbidity and dynamic light scattering. *Anal. Biochem.* **192**:334–343 (1991).
25. F. J. Szoka, F. Olson, T. Heath, W. Vail, E. Mayhew, and D. Papahadjopoulos. Preparation of unilamellar liposomes of intermediaite size by a combination of reverse phase evaporation and through polycarbonate membranes. *Biochim. Biophys. Acta* **601**: 559–571 (1980).
26. J. P. Kratohvil, W. P. Hsu, M. A. Jacobs, and T. M. Aminabhavi, and Y Mukunoki. Concentration-dependent aggregation patterns

of conjugated bile salts in aqueous sodium chloride solutions. A comparison between sodium taurodeoxycholate and sodium taurocholate. *Colloid Polymer Sci.* **261**:781–785 (1983).
27. K. Meguro, M. Ueno, and K. Esumi. Micelle formation in aqueous media. In M.J. Schick (ed.), *Non Ionic Surfactants. Physical Chemistry,* Marcel Dekker, New York, 1987, pp. 109–183.
28. S. Lesieur, C. Grabielle-Madelmont, M.-T. Paternostre, J. M. Moreau, R. M. Handjani-Vila, and M. Ollivon. Action of octylglucoside on non-ionic monoalkyl amphiphile-cholesterol vesicles study of solubilization mechanism. *Chem. Phys. Lipids* **56**:109–121 (1990).
29. M. Ueno. Partition behavior of a nonionic detergent, octyl glucoside, between membranes and water phases and its effect on membrane permeability. *Biochemistry* **28**:5631–5634 (1989).
30. K. Andrieux, S. Lesieur, M. Ollivon, and C. Grabielle-Madelmont. Methodology for vesicle permeability study by HPLC gel exclusion. *J. Chromatogr. B* **706**:141–147 (1998).
31. K. Andrieux. *Interactions des sels biliaires et des phospholipides: application à la transition vésicule-micelle*, Ph. D. Thesis, Université Paris XI, 3 May 2000.
32. C. Grabielle-Madelmont, A. Hochapfel, and M. Ollivon. Antibiotic – phospholipid interactions as studied by DSC and X-ray diffraction. *J. Phys. Chem.* **103**:4534–4548 (1999).
33. P. Walde, J. Sumamoto, and C. J. O'Connor. The mechanism of liposomal damage by taurocholate. *Biochim. Biophys. Acta* **905**: 30–38 (1987).
34. H. Saito, Y. Sugimoto, R. Tabeta, R. Suzuki, G. Izumi, M. Kodama, S. Toyoshima, and Ch. Nagata. Incorporation of bile acid of low concentration into model and biological membranes studied by 2H and 31P NMR. *J. Biochem. (Tokyo)* **94**:1877–1887 (1983).
35. K. Müller. Structural dimorphism of bile salt/lecithin mixed micelles: a possible regulatory mechanism for cholesterol solubility in bile? X-ray structure analysis. *Biochemistry* **20**:404–414 (1981).
36. M. A. Long, E. W. Kaler, and S. P. Lee. Stuctural characterization of the micelle-vesicle transition in lecithin-bile salt solutions. *Biophys. J.* **67**:1733–1742 (1994).
37. C. Tanford. *The Hydrophobic Effect: Formation of Micelles and Biological Membranes*, Wiley, New York, 1973, chap. 10.
38. R. Schubert and K. H. Schmidt. Structural changes in vesicle membranes and mixed micelles of various lipid compositions after binding of different bile salts. *Biochemistry* **27**:8787–8794 (1988).
39. G. A. Kossena, B. J. Boyd, C. J. Porter, and W. N. Charman. Separation and characterization of the colloidal phases produced on digestion of common formulation lipids and assessment of their impact on the apparent solubility of selected poorly water-soluble drugs. *J. Pharm. Sci.* **3**:634–648 (2003).